# Locating the Gribov horizon

Fei Gao,[1] Si-Xue Qin,[2] Craig D. Roberts,[3] and Jose Rodríguez-Quintero[4]
[1]Department of Physics and State Key Laboratory of Nuclear Physics and Technology, Peking University, Beijing 100871, China
[2]Department of Physics, Chongqing University, Chongqing 401331, People's Republic of China
[3]Physics Division, Argonne National Laboratory, Argonne, Illinois 60439, USA
[4]Departamento de Física Aplicada, Facultad de Ciencias Experimentales, Universidad de Huelva, Huelva E-21071, Spain

(Received 14 June 2017; published 8 February 2018)

We explore whether a tree-level expression for the gluon two-point function, supposed to express effects of an horizon term introduced to eliminate the Gribov ambiguity, is consistent with the propagator obtained in simulations of lattice-regularized quantum chromodynamics (QCD). In doing so, we insist that the gluon two-point function obey constraints that ensure a minimal level of consistency with parton-like behavior on the ultraviolet domain. In consequence, we are led to a position which supports a conjecture that the gluon mass and horizon scale are equivalent emergent mass-scales, each with a value of roughly 0.5 GeV; and wherefrom it appears plausible that the dynamical generation of a running gluon mass may alone be sufficient to remove the Gribov ambiguity.

DOI: 10.1103/PhysRevD.97.034010

## I. INTRODUCTION

When quantizing continuum chromodynamics, a gauge fixing condition must be imposed upon the gluon fields. Except in particular cases [1–9], that cannot be completed consistently without adding ghost fields to the Lagrangian [10]. The classical theory's gauge invariance is then replaced by BRST symmetry [11,12], which can be used in perturbation theory to prove, e.g., renormalizability of quantum chromodynamics (QCD). Typically, however, the auxiliary condition meant to select a unique element from each class of equivalent configurations (a gauge field orbit) is nonperturbatively inadequate [1–9]. An unknown (probably infinite) number of configurations remain, each related to the identified element by a nonperturbative gauge transformation, and all contributing equally to the integral that should define the theory. This impedes a rigorous mathematical formulation of QCD; and hence the domain of gauge field integration must be restricted further [1,3].

Contemporary efforts to realize a gauge fixing procedure that selects a unique configuration from each gauge field orbit are described in Ref. [13]. The analysis is typically undertaken in Landau gauge, because, e.g., it is a linear covariant gauge, a fixed point of the renormalization group, and readily implemented in lattice-QCD. Prominent amongst associated schemes is a modification of the standard QCD action to include an "horizon term,"

$$\gamma \int d^4x h(x), \tag{1}$$

$h(x) = g^2 f^{abc} A^b_\mu(x) [\mathcal{M}^{-1}]^{ad}(x,x) f^{dec} A^e_\mu(x)$, where $g$ is the coupling, $\{A^a_\mu\}$ represents the gluons, and

$$\mathcal{M}^{ab}(x,y) = [-\partial^2 \delta^{ab} + \partial_\mu f^{abc} A^c_\mu(x)] \delta^4(x-y) \tag{2}$$

is the Landau gauge Faddeev-Popov operator. The scale $\gamma$ is fixed via the "horizon condition,"

$$\langle h[\gamma] \rangle = d(N^2-1), \tag{3}$$

where the product $d(N^2-1)$, $d=4$, $N=3$, is the number of components of the gluon field, and the expectation value indicates gauge-field integration in the presence of $\gamma$. (Issues of BRST (a-)symmetry, renormalizability, etc., of such an action are canvassed elsewhere [13,14].)

The procedure just described ensures that only those solutions of the Landau-gauge auxiliary condition which produce non-negative values for the Faddeev-Popov determinant ($Det\mathcal{M} \geq 0$) contribute in the gauge-field integration; i.e., it restricts the integration to those Landau-gauge configurations which lie within the so-called first Gribov region, $\Omega$, whose boundary, $\delta\Omega$, the "Gribov horizon," is defined by Landau-gauge configurations for which

$Det\mathcal{M} = 0$. The first Gribov region has significant properties [13]: $\Omega$ contains the trivial $A^0_\mu \equiv 0$ configuration, so a connection with perturbation theory is maintained. It is intersected by each gauge orbit at least once and is convex and compact. It follows that all gauge orbits are represented by configurations within $\Omega$ and any set of Gribov copies within $\Omega$ is bounded.

The procedure summarized here refines the original scheme [10], and its implementation capitalizes on a finding [15] that one may equivalently define the first Gribov region to be the set of relative minima of the functional

$$F_A[U] = \frac{1}{2}\int d^4x [A^a_\mu(x)]_U [A^a_\mu(x)]_U, \tag{4}$$

where $[A^a_\mu]_U$ is a gauge transformation of the field $A^a_\mu$ and the minimization proceeds by choosing those configurations on each orbit which minimize this norm. Plainly, there can be more than one relative minima, and the set of gauge-equivalent minima identifies the Gribov copies tied to a given configuration. From this perspective, the Landau-gauge ambiguity is resolved if the gauge field integration is restricted to those configurations for which $F_A[U]$ is an absolute minimum. The domain of such configurations defines the fundamental modular region, $\Lambda \subset \Omega$, and quantization of QCD may then properly be achieved by integrating only over $A^a_\mu \in \Lambda$. However, an issue remains [8]: no practical, local scheme has yet been devised to achieve this restriction in continuum QCD.

Our discussion highlights that the Gribov horizon, $\delta\Omega$, might play an important role in rigorously defining the scope of gauge sector interactions. Its existence is imposed via $\gamma > 0$ in Eq. (1), whose value is dynamically determined; and known to have the potential to modify the infrared (IR) behavior of the gluon two-point Schwinger function [16]. Hence, writing $g^2\gamma = m^4_\gamma$, one may identify $m_\gamma$ as an interaction-induced mass scale whose value characterizes the location of the Gribov horizon.

Implemented as described, the gauge-fixed action is nonlocal because it involves $\mathcal{M}^{-1}$. At the cost of introducing additional fields, an equivalent local action can be derived, yielding a tree-level gluon propagator for a theory whose gauge fields all lie within $\Omega$ [1,3],

$$D^\gamma_{\mu\nu}(k) = T_{\mu\nu}(k)\mathcal{D}^\gamma(k^2), \quad \mathcal{D}^\gamma(k^2) = \frac{k^2}{k^4 + 2Ng^2\gamma}, \tag{5}$$

$T_{\mu\nu}(k) = \delta_{\mu\nu} - k_\mu k_\nu/k^2$. It is now plausible to suppose that Eq. (5) expresses the dominant IR features of the gluon propagator and hence the scheme employed could be validated through comparison with Landau-gauge lattice-QCD (lQCD) results for this Schwinger function. The most striking feature of Eq. (5) is that $\mathcal{D}^\gamma(k^2) \to 0$ as $k^2 \to 0$ and it is now clear that such behavior is not found in QCD. Instead, the gluon is characterized by a dynamically generated IR mass-scale, which ensures the gluon dressing function is nonzero and finite at $k^2 = 0$ [17–31]. One must, therefore, conclude that the scheme of Refs. [1,3] is incomplete.

A modification to the gauge-fixing scheme of Refs. [1,3] is canvassed in Refs. [21,32] (Other procedures are described in Refs. [33,34].). It admits the possibility that the ghost fields used to localize the horizon term develop a nonzero dimension-two condensate, whose presence further modifies the gluon propagator [21,32]:

$$\mathcal{D}^\gamma(k^2) \to \bar{\mathcal{D}}(k^2) = \frac{k^2 + M^2}{k^4 + k^2\mathfrak{m}^2 + \lambda^4}, \tag{6}$$

where $\lambda^4 = 2Ng^2\gamma - \mu^2M^2$, $\mathfrak{m}^2 = M^2 - \mu^2$, with $\mu^2 \propto \langle A^a_\mu A^a_\mu\rangle$ and $M^2$ related to the ghost-field condensate, both computed within an hadronic medium [35]. Following this method, which supports a nonzero value for the gluon propagator in the far-IR, one can obtain fair agreement with lQCD results for the gluon two-point function [36–38]. Herein, we revisit this issue, using lattice simulations to constrain the parameters in Eq. (6) after imposing novel constraints, and this enables us to develop new insights into their implications and meaning.

## II. PARTONIC CONSTRAINTS

Owing to asymptotic freedom, and notwithstanding confinement and dynamical chiral symmetry breaking, the scalar functions characterizing any one of the two-point Schwinger functions associated with QCD's elementary excitations can be defined as positive on $k^2 \in [0, \infty)$ and must then be convex-down and fall no faster than $1/k^2$, with modest logarithmic corrections, on $\mathcal{P} = \{k^2 | k^2 > k^2_{\mathcal{P}}, \text{for some } k^2_{\mathcal{P}} > \Lambda^2_{\rm QCD}\}$. Denoting such a function by $\mathcal{S}(k^2)$, then equally, as may be shown using the operator product expansion [39], $\exists x_{\mathcal{P}} < 1/\Lambda_{\rm QCD}$ such that $\mathfrak{s}(x^2)$, the four-dimensional configuration space dual of $\mathcal{S}(k^2)$, is convex-down on $\mathcal{P}_x = \{x^2 | 0 < x^2 < x^2_{\mathcal{P}}\}$. These observations simply express the feature that a perturbation theory is valid in the neighborhood of QCD's conformal limit, irrespective of whether that limit is defined in configuration or momentum space. Consequently, only those duals which satisfy this reciprocal relationship can be identified with the theory.

The point is readily illustrated using free-parton propagators, *viz.* writing $\mathcal{S}_f(k^2) = 1/(k^2 + \nu^2)$, with $\nu$ being the parton's mass, and $\mathfrak{x} = \sqrt{x^2}$,

$$\mathfrak{s}_f(\mathfrak{x}) = \int \frac{d^4k}{(2\pi)^4} e^{ik\cdot x}\mathcal{S}_f(k^2) \tag{7a}$$

$$= \frac{1}{4\pi^2}\frac{1}{\mathfrak{x}}\int_0^\infty dk k^2 \frac{J_1(k\mathfrak{x})}{(k^2 + \nu^2)} \tag{7b}$$

$$= \frac{1}{4\pi^2}\frac{\nu}{\mathfrak{x}} K_1(\nu\mathfrak{x}), \tag{7c}$$

where $J_1$ is a Bessel function of the first kind and $K_1$ a modified Bessel function of the second kind. It is important to highlight here that although the parton mass is an infrared parameter, it evidently influences the ultraviolet behavior of the propagator, in both momentum and configuration spaces. The general nature of this phenomenon is exemplified in the role of $\Lambda_{\rm QCD}$: it is QCD's definitive infrared scale and yet it prescribes the evolution of all quantities on the ultraviolet domain.

An elementary correlator that is consistent with perturbative QCD, i.e., possesses a partonic interpretation in the ultraviolet, should, *inter alia*, possess a real, positive effective mass [40–42]. In dealing with simple states, that mass is easily read from either the associated momentum- or configuration-space Schwinger function. It may equally be obtained via the following mathematical procedure, which extracts the system's rest-frame energy:

$$\text{rest mass} = 2\frac{d^2}{d\tau^2}\sigma(\tau)\Big|_{\tau=0}, \tag{8a}$$

$$\sigma(\tau) = \int d^3\vec{x}\,\mathfrak{s}(\mathfrak{x}) \tag{8b}$$

$$= \frac{1}{\pi}\int_0^\infty dk\mathcal{S}(k^2)\cos(\tau k). \tag{8c}$$

Here, $\sigma(\tau)$ is the one-dimensional configuration-space dual of the momentum-space Schwinger function, which, e.g., is the type of object studied in numerical simulations of lattice-regularized QCD in order to extract hadron masses. Importantly, Eqs. (8b) and (8c) are strictly equivalent mathematical definitions of $\sigma(\tau)$ and either may therefore be used to compute the result. It is worth remarking that the operation which delivers the one-dimensional configuration space dual merely sets-to-zero three components of the four-vector $k$ before the transform is computed; and in an O(4)-invariant theory, no direction is preferred in this operation—all directions are equivalent, so the meaning of $d^3\vec{x}$ is simply a convention. A straightforward example is once again obtained with free parton propagators, in which case

$$\sigma_f(\tau) = \int d^3\vec{x}\,\mathfrak{s}_f(\sqrt{\vec{x}^2+\tau^2}) = \frac{1}{2\nu}e^{-\nu\tau}, \tag{9}$$

and Eq. (8a) yields rest mass $= \nu$.

In Eqs. (8), (9), one has an illustration of a general result. Namely, for any system that possesses a partonic interpretation in the ultraviolet, the one-dimensional configuration-space dual of its momentum-space Schwinger function is convex down on the neighborhood $\tau \simeq 0$. (Additional remarks are supplied in the Appendix.)

We now proceed to elucidate the impact of the convexity requirements (partonic constraints) on $\bar{\mathcal{D}}(k^2)$ by considering its one-dimensional configuration space dual,

$$\Delta(\tau) = \frac{1}{\pi}\int_0^\infty dk\cos(\tau k)\bar{\mathcal{D}}(k^2) \tag{10}$$

$$= \Delta_{\mathcal{P}}(\tau)[(1+M^2/\lambda^2)s_{\varphi/2}\cos(\tau\lambda s_{\varphi/2}) - (1-M^2/\lambda^2)c_{\varphi/2}\sin(\tau\lambda s_{\varphi/2})], \tag{11}$$

where $\Delta_{\mathcal{P}}(\tau) = \exp(-\tau\lambda c_{\varphi/2})/(2\lambda s_\varphi)$, $s_\varphi = [1-c_\varphi^2]^{1/2}$, $s_{\varphi/2} = [1-c_{\varphi/2}^2]^{1/2}$, $c_\varphi = \cos\varphi = \mathfrak{m}^2/(2\lambda^2)$, $c_{\varphi/2} = \cos\frac{1}{2}\varphi = [\frac{1}{2}+\mathfrak{m}^2/(4\lambda^2)]^{1/2}$. [The four-dimensional dual is presented in Eq. (A3).]

The Schwinger function in Eq. (6) is that of a massive excitation. Consequently, as we have explained, a propagator consistent with the partonic constraint would possess a one-dimensional dual that behaves as $\exp(-\text{mass}\times\tau)$ on $\tau \simeq 0$. This weak constraint is satisfied if

$$M^2 = \lambda^2, \qquad \lambda^2 \geq \frac{1}{3}\mu^2 \quad \text{(weak)}, \tag{12}$$

for then $\Delta(\tau)|_{M=\lambda} \approx [\exp(-\nu\tau)/(2\nu)][1-\frac{1}{2}\tau^2\lambda^2 s_{\varphi/2}^2]$, $\nu = \lambda c_{\varphi/2}$. Notably, Eq. (12) also ensures that, treated as a polynomial in $\kappa = k^2$, the zeros of the denominator in Eq. (6) possess a nonzero imaginary part.

Of course, a necessary and sufficient condition for true convexity on $\tau \simeq 0$ is that $\Delta''(\tau) > 0$, and

$$\frac{d^2}{d\tau^2}\Delta(\tau)\Big|_{\tau=0} = \frac{\lambda}{4c_{\varphi/2}}[1-\mu^2/\lambda^2], \tag{13}$$

which is positive so long as

$$\mu^2 \leq \lambda^2 \quad \text{(strong)}. \tag{14}$$

## III. INTERPRETING LATTICE-QCD RESULTS

We now explore the impact of the partonic constraints in Eqs. (12), (14) on the description of lQCD results for the gluon two-point function using Eq. (6).

To proceed, we assume that at some renormalization scale, $\zeta_{\rm GZ}$, $\bar{\mathcal{D}}(k^2;\zeta_{\rm GZ}^2) \coloneqq \bar{\mathcal{D}}(k^2)$ in Eq. (6) is a valid representation of that part of the full gluon two-point function which is essentially nonperturbative. There is then a domain of IR momenta, $k^2 \in [0, k_0^2]$, with $k_0$ to be determined, whereupon Eq. (6) should be capable of describing the lQCD propagator, $D_\#$, computed at a known renormalization scale, $\zeta_\#$, after they are both evolved to a common point $\zeta_0 \sim 1$ GeV, typical of hadron physics. On

$k^2 > k_0^2$, the usual logarithms and anomalous dimensions will be generated by renormalization. Since they are absent from Eq. (6), this formula must thereupon fail.

The gluon two-point function is multiplicatively renormalizable, so this perspective can be expressed thus,

$$\forall k^2 \in [0, k_0^2]: \bar{\mathcal{D}}(k^2; \zeta_0^2) = D_{\#}(k^2; \zeta_0^2), \tag{15a}$$

$$\bar{\mathcal{D}}(k^2; \zeta_0^2) = \mathcal{Z}_0(\zeta_0^2, \zeta_{\rm GZ}^2)\bar{\mathcal{D}}(k^2; \zeta_{\rm GZ}^2), \tag{15b}$$

$$D_{\#}(k^2; \zeta_0^2) = D_{\#}(k^2; \zeta_{\#}^2)/[\zeta_0^2 D_{\#}(\zeta_0^2; \zeta_{\#}^2)], \tag{15c}$$

where $\mathcal{Z}_0$, $k_0$ are fit parameters. We will judge the interpretation reasonable so long as $\mathcal{Z}_0 \sim 1$, $k_0 \sim 1$ GeV, in which event it is natural to identify $\zeta_0 = k_0$. There are five parameters: $\mathcal{Z}_0$, $k_0 = \zeta_0$, and $M$, $\mu$, $\lambda$ in Eq. (6). They are determined simultaneously by minimizing the rms relative-difference between the two sides of Eq. (15a) for a given value of $k_0^2$, then optimizing $k_0^2 \in [0, k_{\rm max}^2]$ by seeking that value which produces the global minimum for this rms relative-difference, where $k_{\rm max}$ is the largest momentum at which lQCD results are available.

We first analyze the large-volume quenched simulations in Ref. [23] ($\zeta_{\#} = 4.3$ GeV, $k_{\rm max} = 4.5$ GeV), wherewith our procedure yields the results in Table I A. For this purpose, the $64^4$ and $80^4$ lattices are indistinguishable [38]: we use the latter. Row 1 reports the coefficients that achieve a best fit on the entire domain of available lattice momenta, i.e., $k_0 := k_{\rm max}$, unvaried, with $\zeta_0$ fixed at the value found to produce the global minimum when $k_0$ is optimized, *viz.* determined in producing row 2. The fit's quality is apparent in Fig. 1(a): the ultraviolet (UV) behavior is represented well at the cost of a poorer description of the IR. This is unsurprising, given the preponderance of UV lattice results in the sample domain; and, consequently, $\mathcal{Z}_0$ deviates greatly from unity, indicating that on $k^2 \in [0, k_{\rm max}^2]$ the lQCD output possesses material perturbative contributions, which cannot be captured by Eq. (6). The fit nevertheless exhibits an IR inflection point [at $k_{\rm ip}^2 = (0.36\ {\rm GeV})^2$], signaling that the spectral function associated with this propagator is not positive-definite. Such behavior is widely interpreted as an indicator of confinement [40,42–54]. It is expressed in $\Delta(\tau)$ of Eq. (11) via a nonterminating series of zeros, with the first located at $\tau_{\rm z} = 1.04$ fm: at this scale, even the most tenuous connection with partonic behavior is lost. (Such inflection points and zeros are listed in Table I C.)

Row 2 in Table I A lists the coefficients obtained when fitting the quenched results on $k^2 \in [0, k_0^2]$ Here, $\mathcal{Z}_0$ is closer to unity, so an interpretation using Eq. (6) is more credible. The result is the dot-dashed (green) curve in Fig. 1(a). Here, $k_{\rm ip}^2 = (0.46\ {\rm GeV})^2$ and the first zero in $\Delta(\tau)$ lies at $\tau_{\rm z} = 0.99$ fm; but, notably, neither the weak nor strong condition for partonic behavior is satisfied, and

TABLE I. Panel A: Analysis of large-volume quenched lQCD results [23] ($\zeta_{\#} = 4.3$ GeV, $k_{\rm max} = 4.5$ GeV) using the two-point function in Eq. (6). Row 1: unconstrained fit using simulation results on the entire available domain, $k_0 = k_{\rm max}$. Row 2: unconstrained fit on an IR domain. Row 3: fit respecting the weak parton condition, Eq. (12). Row 4: fit respecting the strong parton condition, Eq. (14), imposing the upper bound. Row 5: fit respecting Eq. (14) and requiring $m_\gamma = m_g$ (see Sec. V). Panel B: As Panel A, but for unquenched results ($N_f = 4$) [43]. Panel C: $k_{\rm ip}^2$—position of the inflection point in $\bar{\mathcal{D}}(k^2; \zeta_0^2)$ when computed using the coefficients listed in the rows above, e.g., A1 means panel A, row 1; $\tau_{\rm z}$—location of the first zero in the associated $\Delta(\tau)$; $\tau_{\rm F}$—related parton-persistence or fragmentation length. (All dimensioned quantities in GeV, except $\tau_{\rm z}$, $\tau_{\rm F}$, in fm.)

| (A) quenched | $k_0$ | $\zeta_0$ | $\lambda$ | $M$ | $\mathcal{Z}_0$ | $M/\lambda$ | $\mu/\lambda$ |
|---|---|---|---|---|---|---|---|
| Unconstrained | 4.5 | 1.1 | 0.84 | 2.10 | 0.43 | 2.49 | 2.33 |
| | $\zeta_0$ | 1.1 | 0.72 | 1.09 | 0.75 | 1.50 | 1.27 |
| Weak | $\zeta_0$ | 1.0 | 0.59 | 0.59 | 1.04 | 1 | 0.45 |
| Strong | $\zeta_0$ | 1.0 | 0.68 | 0.88 | 0.84 | 1.29 | 1 |
| Str + $m_\gamma = m_g$ | $\zeta_0$ | 1.0 | 0.67 | 0.84 | 0.87 | 1.26 | 0.94 |

| (B) unquenched | $k_0$ | $\zeta_0$ | $\lambda$ | $M$ | $\mathcal{Z}_0$ | $M/\lambda$ | $\mu/\lambda$ |
|---|---|---|---|---|---|---|---|
| Unconstrained | 4.0 | 1.1 | 1.01 | 2.38 | 0.59 | 2.36 | 1.91 |
| | $\zeta_0$ | 1.1 | 0.95 | 1.92 | 0.65 | 2.02 | 1.64 |
| Weak | $\zeta_0$ | 1.0 | 0.65 | 0.65 | 1.20 | 1 | 0.42 I |
| Strong | $\zeta_0$ | 1.0 | 0.87 | 1.34 | 0.93 | 1.54 | 1 |
| Str + $m_\gamma = m_g$ | $\zeta_0$ | 1.0 | 0.80 | 1.07 | 0.89 | 1.34 | 0.71 |

| (C) | A1 | A2 | A3 | A4 | A5 | B1 | B2 | B3 | B4 | B5 |
|---|---|---|---|---|---|---|---|---|---|---|
| $k_{\rm ip}$ | 0.36 | 0.46 | 0.48 | 0.48 | 0.48 | | 0.30 | 0.42 | 0.40 | 0.14 |
| $\tau_{\rm z}$ | 1.04 | 0.99 | 0.96 | 0.97 | 0.97 | | 1.35 | 1.05 | 1.33 | 1.36 |
| $\tau_{\rm F}$ | | | 0.67 | 0.81 | 0.80 | | | 0.66 | 1.17 | 1.02 |

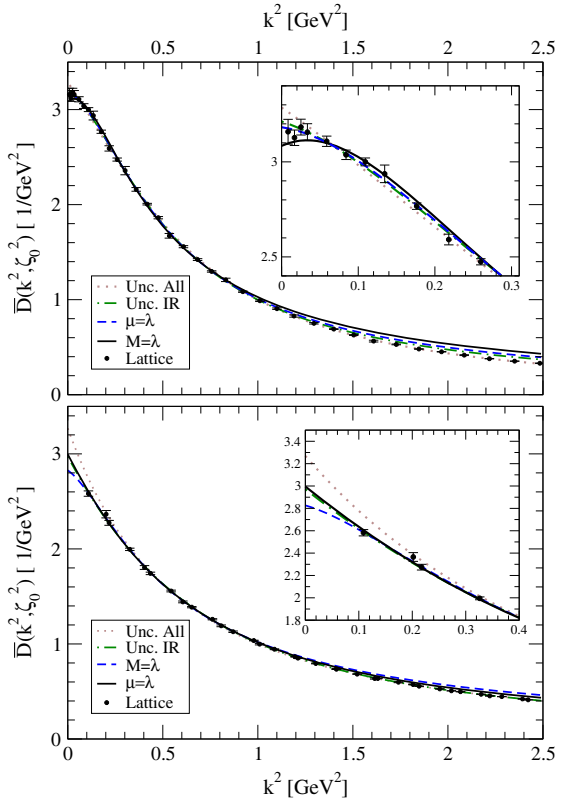


FIG. 1. Upper panel—(a). Fit to quenched lattice results [23], determined as described in connection with Eqs. (15): dotted (brown) curve—row 1 of Table I A, unconstrained, unbounded fit; dot-dashed (green) curve—row 2, Table I A, unconstrained, bounded fit; dashed (blue) curve—row 3, satisfying the weak condition for partonic behavior, Eq. (12); and solid (black) curve—row 4, strong condition, Eq. (14). Lower panel—(b). As upper panel, but for unquenched results ($N_f = 4$) [43]. (The curves and points associated with the unconstrained fits have been rescaled by $(1/1.1)^2$. This eliminates an offset from the constrained results owing to the small difference in optimal scales: $\zeta_0 = 1.1$ GeV *cf.* $\zeta_0 = 1.0$ GeV.)

inspection reveals that $\Delta(\tau)$ has an inflection point at $\tau = 0.078$ fm. Such a striking nonperturbative effect located deep in the UV is in direct conflict with perturbation theory. Hence, this fit, too, should be rejected.

It is appropriate now to describe the fit that respects the weak condition for parton-consistent behavior, Eq. (12): parameters in row 3 of Table I A and dashed (blue) curve in Fig. 1(a). Here, $\mathcal{Z}_0$ is close to unity, and $\bar{\mathcal{D}}(k^2;\zeta_0^2)$ has a global maximum at $k^2 = (0.18\ \mathrm{GeV})^2$ and an inflection point at $k_{\mathrm{ip}}^2 = (0.48\ \mathrm{GeV})^2$. The appearance of a global maximum at $k^2 > 0$ is, perhaps, unexpected, but neither continuum nor lattice studies of QCD's gauge sector can exclude this possibility. In fact, contributions from ghost loops in the gluon vacuum polarization may produce just such an effect [55,56]. It is noteworthy that constraining the behavior of a two-point function on $\tau \simeq 0$, *viz.* a far-UV domain, inaccessible to lattice simulations, enables extraction of more reliable information about this function's behavior at IR momenta, a domain within which lattice results are concentrated. This outcome is a natural inversion of the properties of infrared parameters upon which we remarked following Eqs. (7).

The associated $\Delta(\tau)$ is convex on a domain extending beyond its first zero, $\tau_{\mathrm{z}} = 0.96$ fm. In this instance one may also ask after the persistence of partonic behavior, in which connection we define a fragmentation length as that scale, $\tau_{\mathrm{H}}$, where $\Delta(\tau_{\mathrm{F}})/\Delta_{\mathcal{P}}(\tau_{\mathrm{F}}) = \frac{1}{2}$; i.e., the configuration-space Schwinger function deviates from a partonic propagator by $\geq$50%. Here, $\tau_{\mathrm{F}} = 0.67$ fm.

The fit also yields a value for the "$\langle A^2\rangle$" in-hadron condensate, appearing in the operator product expansion of the gluon two-point function [21,26,36,37,57,58]:

$$g^2\langle A^2\rangle = \frac{32}{3}\mu^2 =: m_{A^2}^2. \tag{16}$$

Phenomenologically, $m_{A^2} \sim (1\text{–}3\ \mathrm{GeV})^2$; but this fit gives $(0.86\ \mathrm{GeV})^2$, as reported in Table II.

Row 4, Table I A specifies the Eq. (14)-consistent fit, which is the solid (black) curve in Fig. 1(a)—little visually distinguishes the results obtained from the weak and strong constraints. Here, $\mathcal{Z}_0$ is close to unity, $k_{\mathrm{ip}}^2 = (0.48\ \mathrm{GeV})^2$, and $\Delta(\tau)$ is convex on a domain extending beyond its first zero, $\tau_{\mathrm{z}} = 0.97$ fm, with $\tau_{\mathrm{F}} = 0.81$ fm.

We now turn to unquenched ($N_f = 4$) results [43] ($\zeta_{\#} = 4.3$ GeV, volume $48^3 \times 96$), with the results listed in Table I B. As evident in Fig. 1(b), there is a paucity of unquenched results at IR momenta, one consequence of which is a need to bound the fitting window in order achieve any reasonable description. Thus, the first row in Table I B lists the coefficients required to achieve a best fit on $k^2 \leq k_{\mathrm{max}}^2$, $k_{\mathrm{max}} = 4.0$ GeV, with $\zeta_0$ fixed at the value found to produce the global minimum when $k_0$ is optimized, *viz.* determined in producing row 2. Owing to the scarcity of results, the fit is poor at IR momenta [see the dotted (brown) curve in Fig. 1(b)] and does not describe a manifestly confined excitation: $\bar{\mathcal{D}}(k^2 > 0;\zeta_0^2)$ has no

TABLE II. Dimension-two condensate, $m_{A^2}$, Eq. (16); gluon mass-scale, $m_g = \lambda^2/M$; and Gribov horizon parameter, $m_\gamma$, Eq. (17), inferred by fitting lattice results using Eq. (6) subject to the parton constraints in Eqs. (12), (14), and also subject to Eq. (14) plus $m_\gamma = m_g$ (see Sec. V). The resolving scale is $\zeta_0 = 1$ GeV. ($\Lambda_{\mathrm{QCD}}^{\mathrm{MOM}(N_f=0)} = 0.425(+15)(-9)$ and $\Lambda_{\mathrm{QCD}}^{\mathrm{MOM}(N_f=4)} = 0.560(\pm 30)$ [57,59,60]. All dimensioned quantities in GeV.)

| | Weak | | | Strong | | | Nec + $m_\gamma = m_g$ | |
|---|---|---|---|---|---|---|---|---|
| $N_f$ | $m_{A^2}$ | $m_g$ | $m_\gamma$ | $m_{A^2}$ | $m_g$ | $m_\gamma$ | $m_{A^2}$ | $m_\gamma = m_g$ |
| 0 | 0.86 | 0.59 | 0.39 | 2.22 | 0.53 | 0.56 | 2.05 | 0.53 |
| 4 | $0.89i$ | 0.65 | 0.40 | 2.84 | 0.56 | 0.75 | 1.85 | 0.60 |

inflection point and $\Delta(\tau \geq 0) > 0$. Furthermore, $\mathcal{Z}_0$ is far from unity because of material perturbative contributions to the lQCD results on this fitting domain.

Row 2, Table I B specifies the fit to unquenched results on $k^2 \in [0, \zeta_0^2]$, $\zeta_0 = 1.1$ GeV. Again, $\mathcal{Z}_0$ is quite different from unity. The result: dot-dashed (green) curve in Fig. 1(b), possesses a first-order inflection point, *viz.* the first $k^2$-derivative of $\bar{\mathcal{D}}(k^2;\zeta_0^2)$ exhibits an inflection point at $k_{\rm ip}^2 = (0.30\ {\rm GeV})^2$, and yields a form for $\Delta(\tau)$ whose first zero lies at $\tau_{\rm z} = 1.35$ fm. Notably, as with the analogous quenched case, neither Eq. (12) nor Eq. (14) is satisfied, and inspection reveals that $\Delta(\tau)$ has an inflection point at $\tau = 0.10$ fm. Hence, this fit is unrealistic.

The impact of the weak condition, Eq. (12), is expressed in row 3, Table I B. Shown as the dashed (blue) curve in Fig. 1(b), it displays an inflection point at $k_{\rm ip}^2 = (0.42\ {\rm GeV})^2$. Computed from there, $\Delta(\tau)$ is convex on a domain that extends beyond its first zero, $\tau_{\rm z} = 1.05$ fm, with $\tau_{\rm F} = 0.66$ fm. Again, imposing a physical constraint on the behavior of a two-point function at far-UV momenta has enabled extraction of more reliable information about its IR behavior. Notwithstanding these features, $|\mathcal{Z}_0 - 1|$ is still too large for us to be confident that the unquenched results are consistent with Eq. (6), especially because $\mu^2 < 1$ and hence $\langle A_\mu^a A_\mu^a \rangle$ has the wrong sign when compared with contemporary phenomenology.

Imposing Eq. (14) (strong) when analyzing the unquenched propagator yields row 4 of Table I B and the two-point function depicted by the solid (black) curve in Fig. 1(b). There is a clear difference between the impact of the weak and strong conditions. The strong condition ensures $\mathcal{Z}_0 \sim 1$ and the fit is characterized by $k_{\rm ip}^2 = (0.40\ {\rm GeV})^2$, $\tau_{\rm z} = 1.33$ fm, and $\tau_{\rm F} = 1.17$ fm.

## IV. GRIBOV HORIZON PARAMETER

Using the coefficients in Table I, one can compute the Gribov horizon scale,

$$m_\gamma^4 := g^2\gamma = \frac{1}{2N}[\lambda^4 + \mu^2 M^2], \tag{17}$$

with the results listed in Table II and compared with the dressed-gluon mass-scale inferred from the same ensembles: $m_g = \lambda^2/M$.

The pattern of the results in Table II is readily explained. For instance, compared with the unquenched values, the sizes of the quenched results are typically smaller owing to the paucity of unquenched IR data, which leads that fit to a focus on UV momenta and thus, usually, increased magnitudes for $\lambda$, $M$, $\mu$. Likewise, the sizes obtained with the weak parton constraint, Eq. (12), are normally smaller than those found with the strong constraint, Eq. (14), because the latter also forces larger magnitudes for $\lambda$, $M$, $\mu$.

Focusing now on the Gribov parameter itself, the weak condition entails $m_\gamma < m_g$, whereas the strong condition favors $m_\gamma \gtrsim m_g$. These outcomes are embedded in Eq. (17), e.g., implementing Eq. (12), one has

$$m_\gamma^4 - m_g^4 \overset{N=3}{=} \frac{\lambda^2}{6}[\mu^2 - 5\lambda^2], \tag{18}$$

which is negative for all values of $\mu^2$ consistent with Eq. (12). On the other hand, enforcing Eq. (14),

$$m_\gamma^4 - m_g^4 \overset{N=3}{\leq} \frac{\lambda^2}{6}\left[\lambda^2 + M^2 - 6\frac{\lambda^6}{M^4}\right]. \tag{19}$$

The rhs is positive $\forall M > 1.24\lambda$, a condition satisfied by all fits except, naturally, those obtained using Eq. (12). Which constraint, then, is more realistic? The value of $m_{A^2}$ suggests the strong condition is better aligned with phenomenology. (The unconstrained fits yield unrealistically large values of $m_{A^2}$.) Notably, for $\mu^2 > 0$, the weak condition always produces a global maximum in $\bar{\mathcal{D}}(k^2;\zeta_0^2)$ at $k^2 > 0$. Hence, a preference for the strong condition places an upper bound on the strength of contributions from ghost loops to the gluon vacuum polarization.

## V. CONCLUSION

Reflecting upon our results, consider that in the context of QCD augmented by the horizon term, Eq. (1), there are three scenarios.

(i) If $g^2\gamma = m_\gamma^4 \gg m_g^4$, then the Gribov horizon affects UV modes of the gluon. The validity of standard perturbation theory shows this is not the case. Consequently, $g^2\gamma \gg m_g^4$ is unrealistic: had it been favored by lQCD results, then it would have been necessary to discard either or both those results and the horizon condition.

(ii) The converse, $m_\gamma \ll m_g$, would have indicated that the gluon mass alone is sufficient to screen IR gluon modes, in which case the Gribov ambiguity could have no physical impact and any horizon term is redundant.

(iii) Our analysis indicates that QCD occupies a middle ground: $m_\gamma \approx m_g$, with each of a size (∼0.5 GeV) that one associates with emergent gauge-sector phenomena. In this scenario, the gluon mass and the horizon scale play a nearly equal role in screening long-wavelength gluon modes, thereby dynamically eliminating Gribov ambiguities. Moreover, together they set a confinement scale of roughly 1 fm, identified with the location of the first zero in the configuration-space gluon two-point function. We therefore conjecture that the gluon mass and horizon condition are equivalent emergent

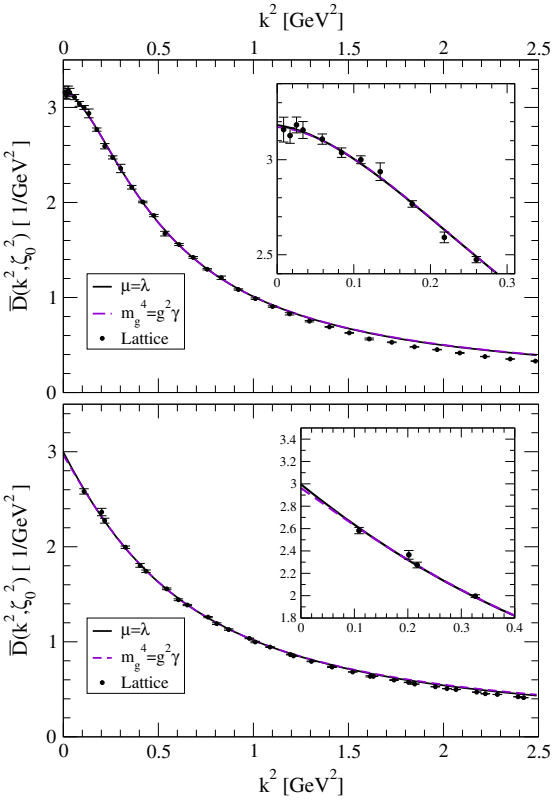


FIG. 2. Upper panel—(a). Dot-dashed (purple) curve fit to quenched lattice results [23], obtained as described in connection with Eqs. (15), imposing Eq. (14) and $m_\gamma = m_g$. (Best-fit coefficients in Table. I.) Solid (black) curve, for comparison, the $\mu = \lambda$ curve from Fig. 1. Lower panel—(b). Same as upper panel, but for unquenched results $(N_f = 4)$ [43].

phenomena. Plainly, unquenched lQCD results with better sensitivity to IR momenta are crucial before anything more can be said with certainty; but if the quenched results are a reasonable guide, then such improvement would increase the likelihood that $m_\gamma = m_g$ is realized.

In the meantime, one can readily check whether $m_\gamma = m_g$ is consistent with available lQCD results, and, as apparent in Fig. 2, that is certainly the case. In this particular realization of scenario (iii), the horizon term, and the $\langle A^2 \rangle$ and ghost-field condensates may all be absorbed into a single running gluon mass, $m_g(k^2)$, whose dynamical appearance alone is then sufficient to eliminate the Gribov ambiguity and complete the definition of QCD.

## ACKNOWLEDGMENTS

We are grateful for insightful comments from D. Binosi, L. Chang, D. Dudal, C. Mezrag and J. Papavassiliou. Research supported by National Natural Science Foundation of China, Contract No. 11435001; National Key Basic Research Program of China, Contracts No. G2013CB834400 and No. 2015CB856900; U.S. Department of Energy, Office of Science, Office of Nuclear Physics, Contract No. DE-AC02-06CH11357; and Spanish MEyC, under Grant No. FPA2014-53631-C-2-P.

## APPENDIX: CONFIGURATION SPACE DUALS

Beginning with the definition of $\sigma(\tau)$ in Eq. (8c), one has

$$\left.\frac{d^2}{d\tau^2}\sigma(\tau)\right|_{\tau=0} = \lim_{\tau\to 0}\frac{d^2}{d\tau^2}\frac{1}{\pi}\int_0^\infty dk\mathcal{S}(k^2)\cos(\tau k) \tag{A1a}$$

$$= \lim_{\tau\to 0}\frac{1}{\pi}\int_0^\infty dk\mathcal{S}(k^2)[-k^2\cos(\tau k)], \tag{A1b}$$

where the step that yields Eq. (A1b) is only valid if the integral converges. Notwithstanding this caveat, a clear point is made by the formal manipulation; *viz.*, the presence of the $k^2$ weighting factor in the integrand emphasizes that the value of $\sigma''(\tau = 0)$ is determined by the ultraviolet behavior of $\mathcal{S}(k^2)$. (Naturally, owing to O(4) invariance, that behavior is insensitive to the orientation of the four-vector $k$.)

This observation is readily illustrated; e.g., consider the following two Schwinger functions:

$$\mathcal{S}_1(k^2) = \frac{1}{k^2+\Lambda_1^2}, \tag{A2a}$$

$$\mathcal{S}_2(k^2) = \frac{1}{k^2+\Lambda_1^2}\frac{\ln[\Lambda_2^2]}{\ln[k^2+\Lambda_2^2]}, \tag{A2b}$$

which, with $\Lambda_1^2 < \Lambda_2^2$, are identical at infrared momenta but differ logarithmically in the ultraviolet. (Any two functions with this property will serve equally well.) It is not difficult to numerically compute the one-dimensional configuration space duals of the functions in Eqs. (A2) and, thus, the second derivatives, which are depicted in Fig. 3. In accordance with the above observation, these duals differ only on the ultraviolet domain, $\tau < 1$. On the configuration-space infrared domain, $\tau > 1$, their behavior is effectively identical because this is also a feature of their momentum-space infrared behavior.

Notably, whilst the functions in Eqs. (A2) are both convex on $k^2 > 0$, their one-dimensional configuration space duals are not. This emphasizes the importance of the partonic constraints we have identified. Evidently, although it is simple to write a model for a Schwinger function that is convex in momentum space, it is nontrivial to build a model that is simultaneously convex on the ultraviolet domain in both momentum and configuration spaces. This means that the partonic constraints serve a real purpose in analyzing models that attempt to relate with QCD. (N.B. It is straightforward to illustrate that there exist classes of ultraviolet-equivalent momentum-space models

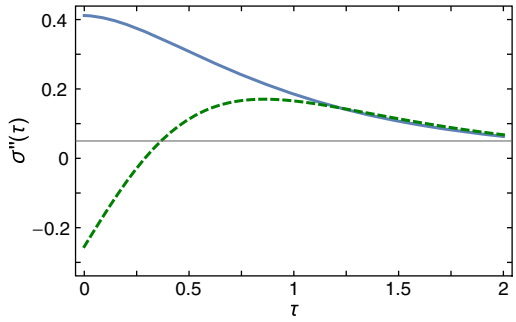


FIG. 3. One-dimensional configurations-space duals of the functions in Eqs. (A2): $\mathcal{S}_1$, solid (blue) curve; and $\mathcal{S}_2$, dashed (green) curve. We used $\Lambda_1 = 1$, $\Lambda_2 = 3$, in arbitrary units.

for which both the momentum and configuration space duals are convex.)

The four-dimensional configuration space dual of the Schwinger function in Eq. (6) is

$$\mathfrak{d}(\mathfrak{x}) = \frac{1}{4\pi^2\mathfrak{x}}\sum_{i=\pm} a_i b_i K_1(\mathfrak{x} b_i), \tag{A3}$$

where, with $\mathfrak{r} = \sqrt{(\mathfrak{m}^2 - 2\lambda^2)(\mathfrak{m}^2 + 2\lambda^2)}$,

$$a_\pm = \frac{\mathfrak{r} \pm \mathfrak{m}^2 \mp 2M^2}{2\mathfrak{r}}, \qquad b_\pm = \frac{1}{\sqrt{2}}(\mathfrak{m}^2 \pm \mathfrak{r})^{1/2}. \tag{A4}$$

$\mathfrak{d}(\mathfrak{x})$ is a real-valued function because $a_\pm$, $b_\pm$ are complex conjugates when $\mathfrak{r}$ possesses an imaginary part, and one readily finds

$$\mathfrak{d}(\mathfrak{x}) \overset{\mathfrak{x}\simeq 0}{\approx} \frac{1}{4\pi^2\mathfrak{x}^2}, \tag{A5}$$

which is identical to the $\mathfrak{x} \simeq 0$ behavior of the free-parton dual in Eq. (7). The rest-mass associated with this parton is not manifest in Eq. (A3). It becomes apparent via Eq. (8b). Given the asymptotic properties of the modified Bessel function $K_1$, the integral does exist, and the result is given in Eq. (11). Naturally, it is the same irrespective of whether one uses Eq. (8b) or (8c), but more easily obtained using the latter.


[1] V. N. Gribov, Nucl. Phys. **B139**, 1 (1978).
[2] W. Konetschny, Phys. Lett. B **90**, 263 (1980); **115**, 503(E) (1982).
[3] D. Zwanziger, Nucl. Phys. **B323**, 513 (1989).
[4] L. Baulieu and D. Zwanziger, Nucl. Phys. **B193**, 163 (1981).
[5] H. S. Chan and M. B. Halpern, Phys. Rev. D **33**, 540 (1986).
[6] J. C. Vink and U.-J. Wiese, Phys. Lett. B **289**, 122 (1992).
[7] P. O. Bowman, U. M. Heller, and A. G. Williams, Phys. Rev. D **66**, 014505 (2002).
[8] A. G. Williams, Prog. Theor. Phys. Suppl. **151**, 154 (2003).
[9] J. B. Zhang, P. O. Bowman, R. J. Coad, Urs M. Heller, D. B. Leinweber, and A. G. Williams, Phys. Rev. D **71**, 014501 (2005).
[10] L. D. Faddeev and V. N. Popov, Phys. Lett. B **25**, 29 (1967).
[11] C. Becchi, A. Rouet, and R. Stora, Ann. Phys. (N.Y.) **98**, 287 (1976).
[12] I. V. Tyutin, arXiv:0812.0580.
[13] N. Vandersickel and D. Zwanziger, Phys. Rep. **520**, 175 (2012).
[14] D. Dudal, S. P. Sorella, and N. Vandersickel, Eur. Phys. J. C **68**, 283 (2010).
[15] M. A. L. Capri, D. Dudal, J. A. Gracey, V. E. R. Lemes, R. F. Sobreiro, S. P. Sorella, and H. Verschelde, Phys. Rev. D **72**, 105016 (2005).
[16] D. Zwanziger, Nucl. Phys. **B321**, 591 (1989).
[17] A. C. Aguilar and J. Papavassiliou, J. High Energy Phys. 12 (2006) 012.
[18] A. Cucchieri and T. Mendes, *Proc. Sci.*, LAT2007 (2007) 297.
[19] A. Cucchieri and T. Mendes, Phys. Rev. Lett. **100**, 241601 (2008).
[20] A. Aguilar, D. Binosi, and J. Papavassiliou, Phys. Rev. D **78**, 025010 (2008).
[21] D. Dudal, J. A. Gracey, S. P. Sorella, N. Vandersickel, and H. Verschelde, Phys. Rev. D **78**, 065047 (2008).
[22] S. J. Brodsky and R. Shrock, Phys. Lett. B **666**, 95 (2008).
[23] I. Bogolubsky, E. Ilgenfritz, M. Muller-Preussker, and A. Sternbeck, Phys. Lett. B **676**, 69 (2009).
[24] O. Oliveira and P. Bicudo, J. Phys. G **38**, 045003 (2011).
[25] A. C. Aguilar, D. Binosi, and J. Papavassiliou, Phys. Rev. D **84**, 085026 (2011).
[26] P. Boucaud, J. P. Leroy, A. Le Yaouanc, J. Micheli, O. Pène, and J. Rodríguez-Quintero, Few Body Syst. **53**, 387 (2012).
[27] A. Aguilar, D. Binosi, and J. Papavassiliou, Phys. Rev. D **86**, 014032 (2012).
[28] D. Binosi, L. Chang, J. Papavassiliou, and C. D. Roberts, Phys. Lett. B **742**, 183 (2015).
[29] A. C. Aguilar, D. Binosi, and J. Papavassiliou, Front. Phys. China **11**, 111203 (2016).
[30] A. K. Cyrol, L. Fister, M. Mitter, J. M. Pawlowski, and N. Strodthoff, Phys. Rev. D **94**, 054005 (2016).
[31] D. Binosi, C. Mezrag, J. Papavassiliou, C. D. Roberts, and J. Rodríguez-Quintero, Phys. Rev. D **96**, 054026 (2017).
[32] D. Dudal, S. P. Sorella, N. Vandersickel, and H. Verschelde, Phys. Rev. D **77**, 071501 (2008).

[33] J. A. Gracey, Phys. Rev. D **82**, 085032 (2010).
[34] J. Serreau and M. Tissierb, Phys. Lett. B **712**, 97 (2012).
[35] S. J. Brodsky, C. D. Roberts, R. Shrock, and P. C. Tandy, Phys. Rev. C **85**, 065202 (2012).
[36] D. Dudal, O. Oliveira, and N. Vandersickel, Phys. Rev. D **81**, 074505 (2010).
[37] A. Cucchieri, D. Dudal, T. Mendes, and N. Vandersickel, Phys. Rev. D **85**, 094513 (2012).
[38] D. Dudal, O. Oliveira, and J. Rodríguez-Quintero, Phys. Rev. D **86**, 105005 (2012).
[39] K. G. Wilson, Phys. Rev. **179**, 1499 (1969).
[40] C. D. Roberts, A. G. Williams, and G. Krein, Int. J. Mod. Phys. A **07**, 5607 (1992).
[41] L. C. Hollenberg, C. D. Roberts, and B. H. McKellar, Phys. Rev. C **46**, 2057 (1992).
[42] F. T. Hawes, C. D. Roberts, and A. G. Williams, Phys. Rev. D **49**, 4683 (1994).
[43] A. Ayala, A. Bashir, D. Binosi, M. Cristoforetti, and J. Rodríguez-Quintero, Phys. Rev. D **86**, 074512 (2012).
[44] H. J. Munczek and A. M. Nemirovsky, Phys. Rev. D **28**, 181 (1983).
[45] M. Stingl, Phys. Rev. D **34**, 3863 (1986); **36**, 651(E) (1987).
[46] C. J. Burden, C. D. Roberts, and A. G. Williams, Phys. Lett. B **285**, 347 (1992).
[47] P. Maris, Phys. Rev. D **50**, 4189 (1994).
[48] M. Bhagwat, M. Pichowsky, and P. C. Tandy, Phys. Rev. D **67**, 054019 (2003).
[49] C. D. Roberts, Prog. Part. Nucl. Phys. **61**, 50 (2008).
[50] A. Bashir, A. Raya, S. Sánchez-Madrigal, and C. D. Roberts, Few Body Syst. **46**, 229 (2009).
[51] A. Bashir, A. Raya, and J. Rodríguez-Quintero, Phys. Rev. D **88**, 054003 (2013).
[52] S.-X. Qin and D. H. Rischke, Phys. Rev. D **88**, 056007 (2013).
[53] P. Lowdon, J. Math. Phys. **57**, 102302 (2016).
[54] W. Lucha and F. F. Schöberl, Phys. Rev. D **93**, 056006 (2016).
[55] A. C. Aguilar, D. Binosi, D. Ibañez, and J. Papavassiliou, Phys. Rev. D **89**, 085008 (2014).
[56] D. Binosi, C. D. Roberts, and J. Rodriguez-Quintero, Phys. Rev. D **95**, 114009 (2017).
[57] B. Blossier, P. Boucaud, M. Brinet, F. De Soto, V. Morenas, O. Pène, K. Petrov, and J. Rodríguez-Quintero, Phys. Rev. D **89**, 014507 (2014).
[58] P. Boucaud, A. Le Yaouanc, J. P. Leroy, J. Micheli, O. Pène, and J. Rodríguez-Quintero, Phys. Rev. D **63**, 114003 (2001).
[59] P. Boucaud, F. De Soto, J. P. Leroy, A. Le Yaouanc, J. Micheli, O. Pène, and J. Rodríguez-Quintero, Phys. Rev. D **79**, 014508 (2009).
[60] B. Blossier, P. Boucaud, M. Brinet, F. De Soto, X. Du, V. Morenas, O. Pène, K. Petrov, and J. Rodríguez-Quintero, Phys. Rev. Lett. **108**, 262002 (2012).